TÜBİTAK

Turkish Journal of Earth Sciences

http://journals.tubitak.gov.tr/earth/

Research Article

Turkish J Earth Sci
(2019) 28: 671-686

doi:10.3906/yer-1812-10

Plio-Quaternary stress states along the Kütahya Fault and surroundings, NW Turkey

Elif AKGÜN[1,*], **Süha ÖZDEN**[2]

[1]Department of Geological Engineering, Faculty of Engineering, Fırat University, Elazığ, Turkey

[2]Department of Geological Engineering, Faculty of Engineering, Çanakkale Onsekiz Mart University, Çanakkale, Turkey

Received: 18.12.2018 • **Accepted/Published Online:** 07.05.2019 • **Final Version:** 04.09.2019

Abstract: The Kütahya Fault, which is one of the major neotectonic structures in western Anatolia, Turkey, is an active fault constraining the southern margin of the approximately E–W trending Kütahya Basin between the Eskişehir Fault to the north and the Simav Fault to the south. In the present study, inversion of both fault kinematic analysis of fault-slip data and focal mechanism solutions from the Kütahya Fault and surroundings is used to understand the Late Cenozoic stress states. The fault kinematic analysis result yielded three different stress regimes from Mio-Pliocene to Quaternary. Firstly, strike-slip faulting developed under a NE–SW trending local compressional regime with 51° ± 24° (σ_1) and 140° ± 7° (σ_3) trends and R_m ratio was calculated as 0.61, consistent with this faulting. NW–SE trending consistent extensional direction produced local normal faulting with 144° ± 3° (σ_3) trend. Secondly, strike-slip faulting developed under a NW–SE trending local compressional regime showing 143° ± 17° (σ_1) and 51° ± 10° (σ_3) trends and R_m ratio was calculated as 0.51. Finally actual normal faulting developed under a NNE–SSW trend with a regional extensional direction showing 42° ± 14° (σ_3) and R_m ratio of 0.56 at the present time. Inversion of the earthquakes gives a NNE–SSW extension direction with 21° ± 19° (σ_3) trend and R_m ratio calculated as 0.68 at the triaxial. The Kütahya Fault and surroundings are under an extensional regime at the present time. The reason for the regionally effective NNE–SSW trending extensional regime in western and southwestern Anatolian is complex subduction processes (roll-back, retreat, delamination, slab-tear, slab-break-off and/or slab-pull) of the African Plate and the Anatolian Platelet in the Mediterranean region.

Key words: Inversion, kinematic analysis, Kütahya Fault, earthquake, extension, Anatolia

1. Introduction

The Anatolian Block is an important continental area within the Alpine-Himalaya mountain belt between the Eurasian Plate to the north and the Arabian/African Plates to the south (Figure 1). The continent–continent collision between the Arabian Plate and the Anatolian Block began in Eastern Anatolia in the Late Miocene time (Şengör and Yılmaz, 1981). The result of this collision was shortening, partial thickening, and simultaneous increase in the elevation of the Eastern Anatolia plateau (Şengör et al., 2003). The Anatolian Block was pushed to the west away from this collision along the right lateral North Anatolian Fault (NAF) (Ketin, 1948) and left lateral East Anatolian Fault (EAF) (Arpat and Şaroğlu, 1972). While the compressional regime dominated in Eastern Anatolia, in Western Anatolia the west-moving Anatolian Block was compressed in an E–W direction due to the Hellenic Shear Zone and simultaneously moved toward the subduction zone to the SW and above the African Plate in attempting to escape from the collision to the east and west. In the Aegean, Western, and SW Anatolia region, the kinematic NNE–SSW extension plays a large role in the subduction process between the Anatolian Block and African Plate. The behavior of this subduction zone is directly related to the situation of the African Plate along the Hellenic Arc to the west and the Cyprus Arc to the east. The Gulfs of Corinth and Evian in the west of the Eastern Mediterranean and south of Greece (Roberts and Ganas, 2000), the main opening of the Aegean in the Mediterranean (Zanchi and Angelier, 1993) area, east of the Eastern Mediterranean where the Arabian/African/Anatolian plates intersect, and in the west along the African Plate were formed by developing processes such as roll-back, slab-pull (Jackson and McKenzie, 1988; Mercier et al., 1991; McClusky et al., 2000; Faccenna et al., 2004, 2006; Wdowinski et al., 2006; Jolivet and Brun, 2010; Över et al., 2010, 2013a, 2013b; Jolivet et al., 2013), slab tearing (Wortel and Spakman, 2000; Piromallo and Morelli, 2003; Biryol et al., 2011), and slab-break-off and delamination (Al-Lazki et al., 2003; Piromallo and Morelli, 2003; Mutlu and Karabulut, 2011; Göğüş et al., 2011; Komut et al., 2012). The Anatolia Block overlying the African Plate above this complex subduction

* Correspondence: eliffiratligil@gmail.com

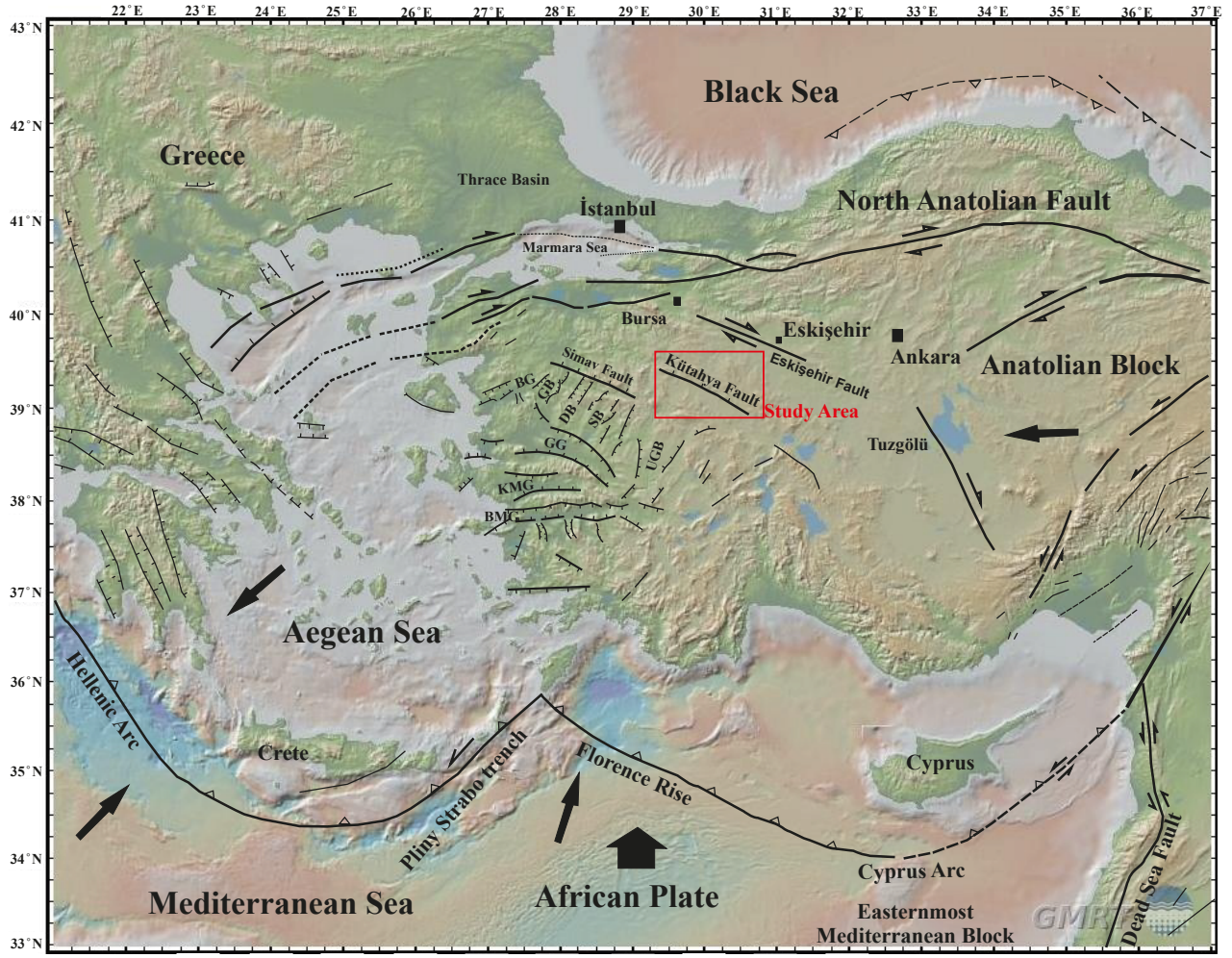

Figure 1. Location of the study area in the main structural units of Western Anatolian surroundings (BG: Bakırçay Graben, GG: Gediz Graben, KMG: Küçük Menderes Graben, BMG: Büyük Menderes Graben, GB: Gördes Basin, DB: Demirci Basin, SB: Selendi Basin, UGB: Uşak-Güre Basin) (modified from Barka, 1992; Bozkurt, 2001; Över et al., 2010).

process rapidly expanded toward the Hellenic and Cyprus arcs (Mercier, 1981; Mercier et al., 1979; Le Pichon and Angelier, 1981; Barka and Reilinger, 1997; Faccenna et al., 2006; Jolivet et al., 2013). Three important models are proposed for this extension: the postorogenic collapse model (Dewey, 1988; Seyitoğlu and Scott, 1991, 1992), the tectonic escape model (Dewey and Şengör, 1979), and southward roll-back of the African slab or the back-arc spreading model (Le Pichon and Angelier, 1979, 1981). Within this process continuing from the Late Miocene to the present day, Western Anatolia was tectonically pulled toward the African Plate and a significant N–S oriented extensional (opening) area was formed. The region, in addition to local compressional periods with uplift, lateral slide deformation, and block rotations, was deformed under a regional extensional regime in the Middle Miocene/Pliocene and Pliocene/Quaternary periods. It became a graben region with fault zones developing with mainly E–W and some N–S, NW–SE, and NE–SW orientations (Dumont et al., 1979, Angelier et al., 1981, Şengör, 1987; Seyitoğlu and Scott, 1991, 1992; Cohen et al., 1995; Koçyiğit et al., 1999; Yılmaz et al., 2000; Alçiçek et al., 2005; Över et al., 2016). Between the nearly E–W oriented faults located in Western Anatolia, from north to south the Eskişehir, Kütahya, and Simav Faults offer significant extension. From deformation on these faults it is known that they did not develop under a single type of tectonic regime.

Currently it is thought that from their formation to the present day they operated under local and regional compressional and extensional regimes. The deformation type in the crust on these types of active faults may be determined from data measured on fault planes and earthquake data. The data obtained can be used to find the

dominant stress tensors, regime types in the region, and stress changes in these regime types along the fault and in surrounding areas from the past to the present.

In the present study for the first time, both data obtained from kinematic analysis of fault assemblages and inversion of the focal mechanism solutions of earthquakes will be used together to determine the local and regional scale stress tensors, stress states, and geodynamic evolution of the region on the Late Cenozoic (Plio-Quaternary) Kütahya Fault (Figure 1) and to interpret the relationships with other structures in the region and especially the situation in west and SW Anatolia.

2. Geology, tectonics, and seismic activity along the Kütahya Fault and surroundings

The study area is examined in two sections: basement and cover rocks. Basement rocks comprise schists at the base, crystallized limestone conformably overlying the schists, and ophiolitic rocks tectonically emplaced as a result of the closure of the İzmir–Ankara–Erzincan suture zone above these rocks. Cover rocks comprise young units, overlying the basement units unconformably (Figure 2). Since the Neogene there has been deposition of conglomerates, sandstone, claystone, marl, limestones, siliceous limestones, and lignite in the region. Additionally effective volcanic activity is noted in the study area. This volcanic activity began at the end of the Miocene and increased in the Pliocene. Lastly all these units are overlain unconformably by Quaternary aged alluvium and travertines (Figure 2).

The Kütahya Fault is the most significant structural element from the neotectonic period (from Late Miocene to recent) in the study area. This fault currently is WNW–ESE oriented with 40 km length. This fault presents clear morphology bounding the southern edge of the Kütahya basin. Between Tavşanlı and west of Kütahya, this active fault has roughly N 80° W orientation and is located mainly between the plain to the north (Kütahya Graben) and immediately in front of the basement units forming uplift to the south (Figure 3). From its formation to the present day the Kütahya Fault affected basement rocks and cover rocks. In the past this fault acted as a strike-slip fault in periods, passing through and affecting especially Lower Pliocene age units. According to the analytical signal map produced from the aeromagnetic data of the study area, the metamorphic massifs with the E–W direction cause magnetic anomalies concentrated in the west and south of Kütahya (Bilim, 2007). The maxspot map derived from the location of the horizontal gradient of aeromagnetic anomalies shows that it is compatible with both tectonic lineaments and the distribution of earthquake data (Bilim, 2007). Currently the Kütahya Fault was transformed to a normal fault recently, forming the boundary between basement units and cover rock and limiting the basin area to half-graben appearance. The fault has its most western end near Tavşanlı and ceases in parallel faults within basement units immediately SW (Figure 3). Many researchers have concluded it is a young and active fault due to fluvial deposits, hanging valleys, alluvial fans, triangular surfaces, and hot springs present along the fault and also current GPS velocities, seismic activity data, and the fact that it cuts Plio-Quaternary aged deposits (Şaroğlu et al., 1992; Barka and Reilinger, 1997; Koçyiğit and Bozkurt, 1997; Özburan, 2009; Altınok et al., 2012; Özburan and Gürer, 2012; Emre et al., 2013). Şaroğlu et al. (1992) mentioned the fault as a normal dip-slip fault due to down-drop of the fault block to the north. However, it is noted that especially in western sections the fault has strike-slip morphology and noting

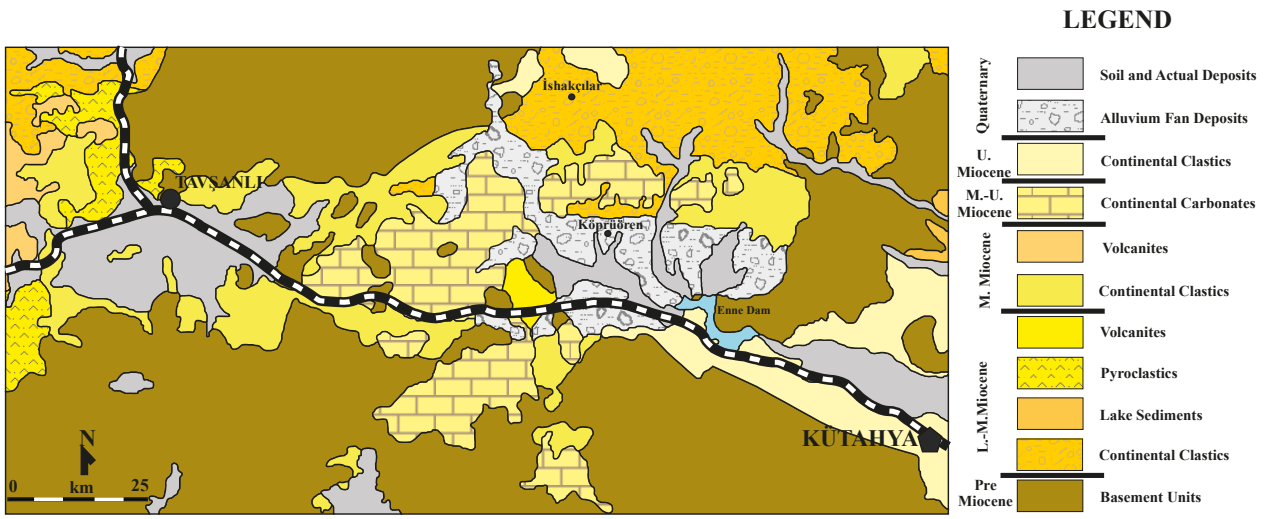

Figure 2. Geological map of the Kütahya Fault and surroundings (modified from Konak, 2002).

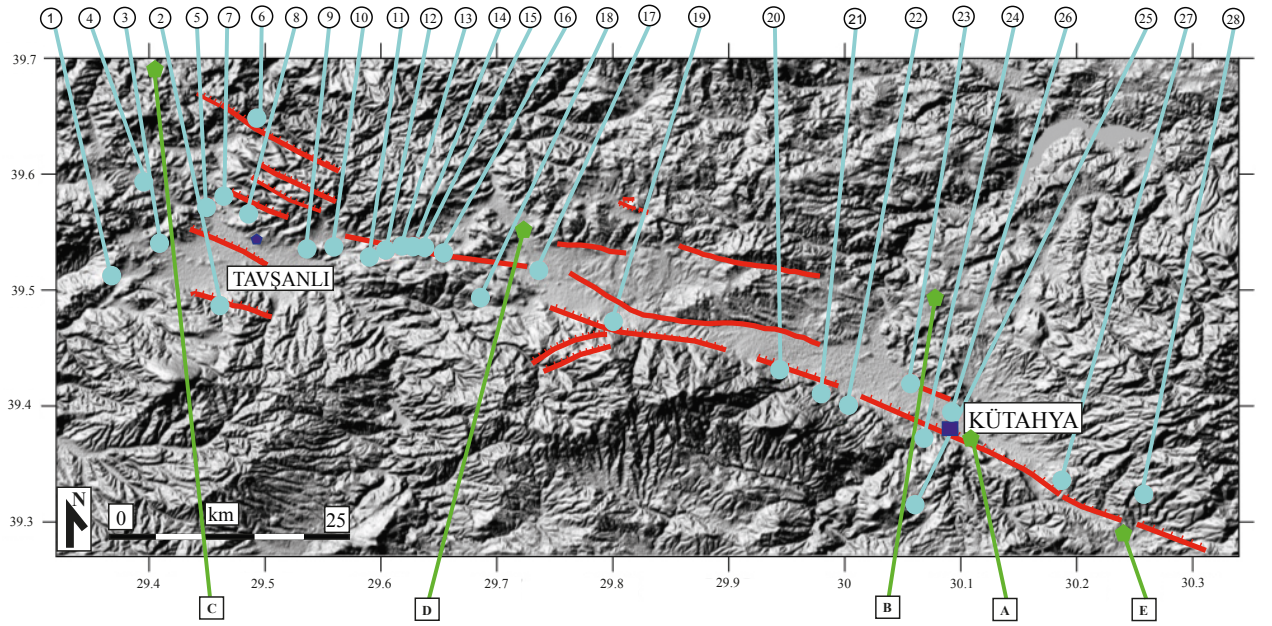

Figure 3. Location DEM map of the sites of the fault kinematic analysis data (numbers/1-28) and earthquakes epicenters (characters/A-E). Red lines represent the faults.

this characteristic it was stated that the fault has a right lateral strike-slip component in addition to dip-slip motion. Gürer et al. (2005) proposed that the Kütahya Fault Zone was a normal fault with a left lateral component. Koçyiğit and Bozkurt (1997) and Bozkurt (2001, 2003) stated that the main characteristic of the Kütahya Fault Zone was that of a normal fault. In our study the Kütahya Fault was identified to begin movement as a left lateral strike-slip fault under a compressional regime and is currently continuing motion as a normal fault under an extensional regime.

There are no definite data for the age of the Kütahya Fault. While Koçyiğit and Bozkurt (1997) recommended the age of the Kütahya Fault as Early Pliocene, Özburan (2009) stated that according to the youngest unit cut by the Kütahya Fault the initiation age of the fault is Early Pleistocene. These age data refer to the period when the fault acted as a normal fault, and do not present any age data for previous behavior.

As a result of the paleoseismological and archaeological studies (Altınok et al., 2012) conducted in the study area, it has been revealed that two devastating earthquakes have occurred on the Kütahya Fault in the last 8000 years with paleoseismological studies, and a slip velocity rate of 0.2 mm/year was calculated on the Kütahya Fault. It has been determined that there is potential for an M > 7.0 earthquake (Altınok et al., 2012).

Ambraseys and Tchalenko (1972) and Koçyiğit (1984) stated that the general trend of the active seismic belt called the Akşehir-Simav Fault Zone south of the study area was parallel to the Kütahya Fault Zone. Koçyiğit and Bozkurt (1997) described this fault system and characteristics as being very similar to the Kütahya Fault Zone. Additionally Tokay and Altunel (2005) stated that the Eskişehir Fault Zone, located north of the study area, was an active fault zone and again explained it was parallel to the Kütahya Fault Zone. Özden et al. (2015) stated that the Eskişehir Fault north of the Kütahya Fault is currently right lateral, while the Simav Fault to the south (Demirci et al., 2015; Gündoğdu et al., 2015; Karasözen et al., 2016; Erkul et al., 2017) displays normal fault (extension) behavior.

Although there has been no destructive earthquake in the study area in the instrumental period, the parallelism and similarity to active faults, and two destructive earthquakes in historical earthquake records along with the observation of active tectonic elements like fault-front deposits along the fault zone (indicator) and hot springs indicate that the Kütahya Fault is an active fault. This fault has the potential to produce earthquakes similar to the Simav Fault (19.11.2011, Mw: 5.8), Eskişehir Fault (20.02.1956, Ms: 6.4), and Eski Gediz Fault (28.03.1970, Mw: 7.0) to the south and north of the study area.

3. Fault kinematic analysis

This study involved kinematic analysis of fault linkage (data sets) along the Kütahya Fault and geological units in near surroundings to determine the main forces, kinematic evolution of the region, and current tectonic regime. Parameters concerning fault planes (fault strike, dip amount, dip direction, altitude values) were measured in the study area.

Two hundred and fifty-five fault planes were measured at 28 stations (Figure 3; Table 1). Faults in geological units with varying ages and lithologies, especially faults in the young period, were used in an attempt to determine the kinematic evolution of the Kütahya Fault in the region from the past to the present day.

3.1. Methodology of fault kinematic analysis

The basis of this study is the kinematic analysis method for fault assemblages developed in the computer environment by Carey-Gailhardis and Mercier (1987) after being proposed by Carey (1979). This method may be used for inverse solutions of focal mechanisms of faults occurring in the region as well as being applicable to faults compiled in the field (Methodology as a detail in Över et al., 2010).

3.2. Fault kinematic analysis results

3.2.1. NE–SW local compressional regime (SS.1a)

According to strike-slip fault plane data measured at stations 8, 10, 11, 17, 22, 24, and 25 in the study area, the largest principle stress axis (σ_1) is σ_1 = 51°/24°, while the smallest principle stress axis (σ_3) is σ_3 = 140°/7°. The Rm ratio was 0.61.

Here the largest principle stress axis (σ_1) and the smallest principle stress axis (σ_3) are horizontal, while the intermediate stress axis (σ_2) is vertical, and so the tectonic regime is strike-slip faulting (Figure 4; Table 2a). These results show the orientation of the compression (σ_1) in the region is N 51° E. The extensional orientation (σ_3) in the region is N 40° W. As the R ratio is larger than 0.55, the

Table 1. Location of fault striae measurement sites with latitude, longitude, altitude, and age of faulted formations.

Station	UTM (Longitude)	UTM (Latitude)	Fault-slip vectors, N	High (Altitude, m)	Age (Geological Unit)	Lithology
1	35S0703437	4376321	12	946	Quaternary	Clastics
2	35S0711734	4373765	11	906	Pre Miocene	Ultrabasics
3	35S0770151	4379468	5	879	Quaternary	Clastics
4	35S0705755	4385416	6	890	Lower Pliocene	Volcanoclastics
5	35S0710437	4383266	7	826	Lower Pliocene	Volcanoclastics
6	35S0713570	4382571	6	877	Lower Pliocene	Volcanoclastics
7	35S0711654	4384107	8	814	Lower Pliocene	Volcanoclastics
8	35S0713811	4391794	9	824	Pre Miocene	Limestone
9	35S0717904	4379450	13	850	Pre Miocene	Ultrabasics
10	35S0719957	4379701	14	905	Pre Miocene	Ultrabasics
11	35S0723890	4379169	7	958	Pre Miocene	Ultrabasics
12	35S0722624	4378866	10	928	Lower Pliocene	Volcanoclastics
13	35S0724928	4379708	15	1041	Lower Pliocene	Volcanoclastics
14	35S0726607	4379814	5	1027	Lower Pliocene	Volcanoclastics
15	35S0728050	4379108	6	1079	Lower Pliocene	Volcanoclastics
16	35S0725995	4379943	17	1019	Lower Pliocene	Volcanoclastics
17	35S0735264	4377836	10	1027	Quaternary	Clastics
18	35S0730951	4374944	7	1018	Upper Pliocene	Limestone
19	35S0740914	4373155	7	1031	Pre Miocene	Limestone
20	35S0753399	4368416	7	998	Lower Pliocene	Pyroclastic
21	35S0763176	4367992	11	1009	Lower Pliocene	Pyroclastic
22	35S0756673	4366711	5	1076	Upper Pliocene	Limestone
23	36S0758703	4365650	8	1003	Upper Pliocene	Limestone
24	35S0764144	4362633	11	974	Upper Pliocene	Limestone
25	36S0763912	4356333	5	1106	Upper Pliocene	Limestone
26	36S0766356	4364736	3	957	Upper Pliocene	Limestone
27	36S0774726	4359051	16	1058	Pre Miocene	Ultrabasics
28	36S0780949	4357868	14	1192	Pre Miocene	Ultrabasics

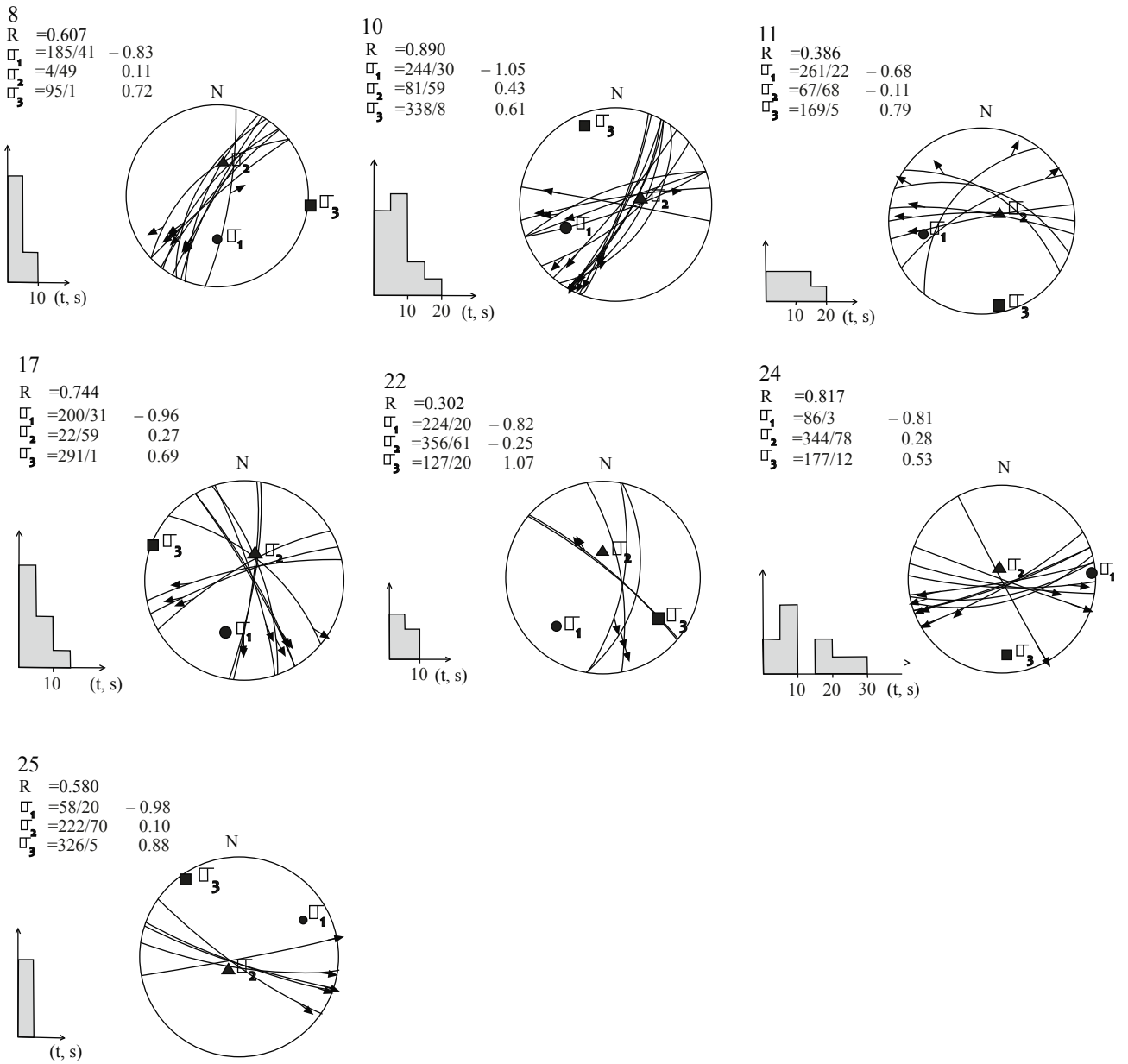

Figure 4. Lower hemisphere stereoplots showing a strike-slip faulting mechanism under NE–SW compressional tectonic regime (SS.1a) results shown in Table 2a. Histogram shows distribution of deviation angles (angle between the observed slip, s, the predicted slip, t).

regime may be said to have a transpressional character.

This main fault behavior displaying left lateral strike-slip movement is observed in limestones in the Tunçbilek area and on fault planes and slip-rake preserved in the Upper Miocene deposits close to Kütahya (Figure 4).

3.2.2. NW–SE local extensional regime (SS.1b)

From stations 1, 23, and 28, data concerning normal faulting were assessed (Figure 5; Table 2b) and the smallest principle stress axis (σ_3) was calculated as σ_3 = 144°/3°. The Rm ratio was 0.26.

Here the smallest principle stress axis σ_3 and intermediate stress axis (σ_2) have horizontal positions, while the largest principle stress axis (σ_1) has a vertical position, representing normal faulting in an extensional regime (Figure 5; Table 2b). These results show the extensional orientation (σ_3) in the region is N 36° W.

The two regime periods explained above are in accordance with limited numbers of outcrops along the length of the Kütahya Fault and were regimes effective before the Late Pliocene.

Table 2. Results of stress tensor inversions for slip data and earthquakes representing (a) SS.1a, (b) SS1b, (c) SS.2 and (d) SS.3-SFM stress regimes.

2a	Station	N	σ_1 Az/dip	σ_2 Az/dip	σ_3 Az/dip	Rm
	8	9	185 / 41	4 / 49	95 / 1	0.60
	10	14	244 / 30	81 / 59	338 / 8	0.89
	11	7	261 / 22	67 / 68	169 / 5	0.38
	17	10	200 / 31	22 / 59	291 / 1	0.74
	22	5	224 / 20	356 / 61	127 / 20	0.30
	24	11	86 / 3	344 / 78	177 / 12	0.81
	25	5	58 / 20	222 / 70	326 / 5	0.58
	SS.1a	61	σ_1 = 51° / 24° and σ_3 = 140° / 7° Rm = 0.61			
2b	Station	N	σ_1 Az/dip	σ_2 Az/dip	σ_3 Az/dip	Rm
	1	12	67 / 71	256 / 19	165 / 3	0.11
	23	8	199 / 81	57 / 7	326 / 5	0.66
	28	14	211 / 86	32 / 4	302 / 0	0.02
	SS.1b	34	σ_3 = 144° / 3° Rm = 0.26			
2c	Station	N	σ_1 Az/dip	σ_2 Az/dip	σ_3 Az/dip	Rm
	3	5	174 / 36	323 / 50	72 / 16	0.22
	4	6	153 / 2	55 / 78	243 / 12	0.66
	5	7	274 / 23	93 / 67	184 / 0	0.26
	6	6	316 / 4	144 / 86	46 / 1	0.73
	9a	7	144 / 25	308 / 65	51 / 6	0.37
	12	10	325 / 19	100 / 64	229 / 17	0.87
	13	15	331 / 24	147 / 66	240 / 1	0.23
	14	5	144 / 9	319 / 81	54 / 1	0.42
	15	6	314 / 4	46 / 35	218 / 55	0.51
	16	17	150 / 9	327 / 81	60 / 0	0.85
	27a	5	170 / 42	340 / 47	75 / 5	0.36
	SS.2	89	σ_1 = 143° / 17° and σ_3 = 51° / 10° Rm = 0.51			
2d	Station	N	σ_1 Az/dip	σ_2 Az/dip	σ_3 Az/dip	Rm
	2	11	328 / 73	143 / 17	233 / 2	0.22
	7	8	331 / 71	116 / 16	209 / 11	0.01
	9b	6	110 / 65	348 / 14	253 / 20	0.94
	18	7	38 / 59	139 / 7	232 / 30	0.67
	19	7	190 / 64	5 / 25	96 / 2	0.32
	20	7	297 / 55	97 / 34	193 / 9	0.93
	21	11	349 / 67	96 / 7	189 / 22	0.72
	26	3	199 / 66	104 / 2	13 / 24	0.49
	27b	11	354 / 81	138 / 7	228 / 5	0.72
	SS.3	71	σ_3 = 42° / 14° Rm = 0.56			
	SFM	5	σ_3 = 21° / 19° Rm = 0.68			

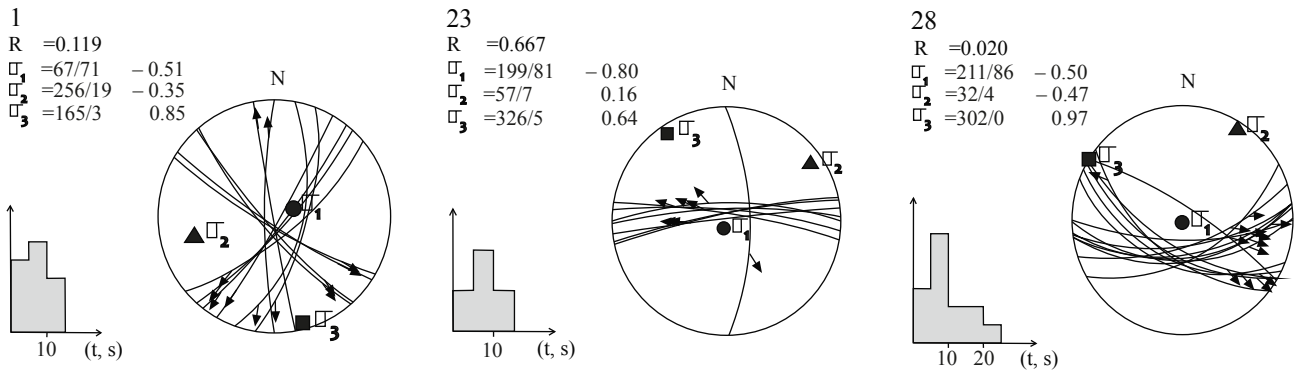

Figure 5. Lower hemisphere stereoplots showing a normal faulting mechanism under NW–SE extensional tectonic regime (SS.1b) results shown in Table 2b. Histogram shows distribution of deviation angles (angle between the observed slip, s, the predicted slip, t).

3.2.3. NW–SE local compressional regime (SS.2)

According to strike-slip data measured at stations numbered 3, 4, 5, 6, 9a, 14, 15, 16, and 27, the largest principle stress axis (σ_1) is σ_1 = 143°/17°, while the smallest principle axis (σ_3) is σ_3= 51°/10°. The Rm ratio was 0.51.

The largest and smallest principle stress axes, σ_1 and σ_3, respectively, have horizontal positions, while the intermediate stress axis (σ_2) has a vertical position, indicating a tectonic regime with strike-slip faulting (Figure 6; Table 2c). These data show the compressional orientation in the region (σ_1) is N 37° W. Accordingly the orientation of the extension (σ_3) is N 51° E.

Under a NW–SE oriented local compressional regime, strike-slip faulting, reverse faults, and folds developed generally in volcanic sandstones. This regime was effective for a short period in the Late Pliocene.

3.2.4. NNE–SSW regional extensional regime (SS.3)

According to data for normal faulting assessed at stations 2, 7, 9c, 12, 13, 18, 19, 20, 21, 26, and 27b (Figure 7; Table 2d), the smallest principle stress axis (σ_3) was σ_3 = 42°/14°. The Rm ratio was 0.56.

Here the smallest principle stress axis (σ_3) and intermediate stress axis (σ_2) have horizontal positions, while the largest principle stress axis (σ_1) has a vertical position, indicating an extensional regime with normal faulting (Figure 7; Table 2d). These data indicate the extensional orientation (σ_3) in the region is N 42° E. This regime is the effective regime after the Late Pliocene, possibly Quaternary, to the present day.

The presence of three effective stress regimes was identified from before the Late Pliocene to the present day for the Kütahya Fault and surrounding area (Figures 4–7; Tables 2a–2d). To determine the correct order of development from the oldest of these regimes to the present day, the presence of slip vectors overlying each other on the same fault plane is helpful (Figure 8). In the study area, in addition to data from many fault planes providing the chronologic order of the tectonic regimes, data especially from stations 12, 20, 23, and 27 were used (Figure 8). Among these, they appear at metric (giant) scale on the main fault plane on a normal fault developing under the last regime represented by NNE–SSW orientation and effective currently (Figure 9) in Evliya Çelebi Neighborhood, forming station number 20. Additionally along the Kütahya Fault most outcrop data provide clear field examples of the NW–SE oriented compressional regime (Figure 10).

3.3. Methodology of focal mechanism solution and inversion of earthquakes

To calculate the stress state for the present day, the population of source mechanisms of earthquakes that occurred along the Kütahya Fault around the Kütahya Basin was examined. Firstly, we performed a moment tensor inversion procedure for some recent earthquakes, namely those with close to surface-observed main faults. For the moment tensor inversion wave form modeling was determined using the source parameters proposed by Dreger's (2002) computer application method. We analyzed the waveforms of the selected 5 earthquakes using the Kandilli Observatory and Earthquake Research Institute's (KOERI) open access data using the software zSacWin. Secondly, the inversion method proposed by Carey-Gailhardis and Mercier (1987) was used including one of several existing algorithms (Methodology as a detail in Özden et al., 2015).

3.4. Focal mechanism solutions and inversion results of the earthquakes

Focal mechanism solutions were completed for 5 earthquakes (A, B, C, D, and E) (Figure 3) occurring between 2004 and 2013 and varying in magnitude from 2.9 to 4.2 (Figure 11; Table 3). While individual focal mechanism solutions for each earthquake indicated normal faulting, the numerical solutions for these earthquakes and beach balls are presented in Table 3 and Figure 11.

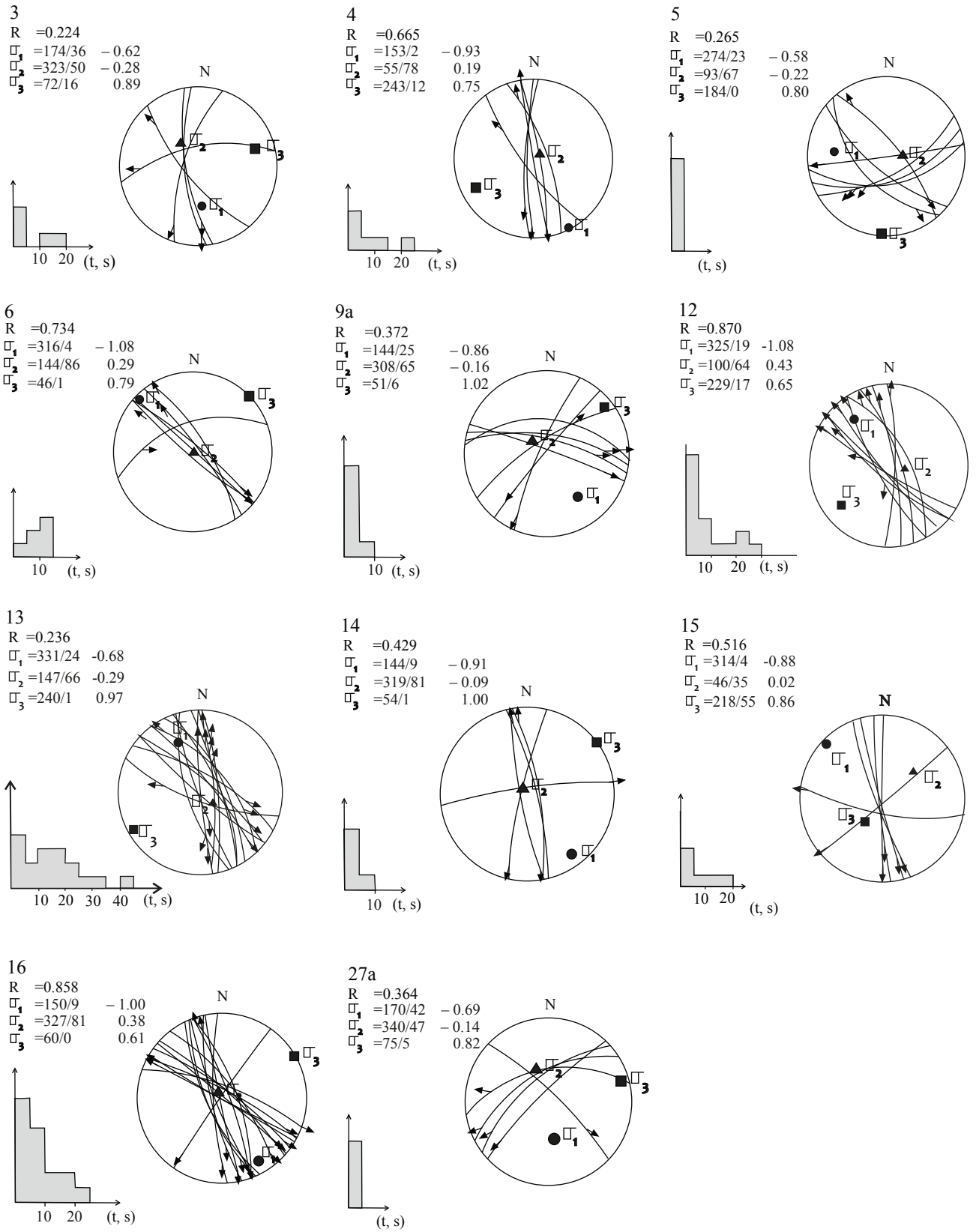

Figure 6. Lower hemisphere stereoplots showing a strike-slip faulting mechanism under NW–SE compressional tectonic regime (SS.2) results shown in Table 2c. Histogram shows distribution of deviation angles (angle between the observed slip, s, the predicted slip, t).

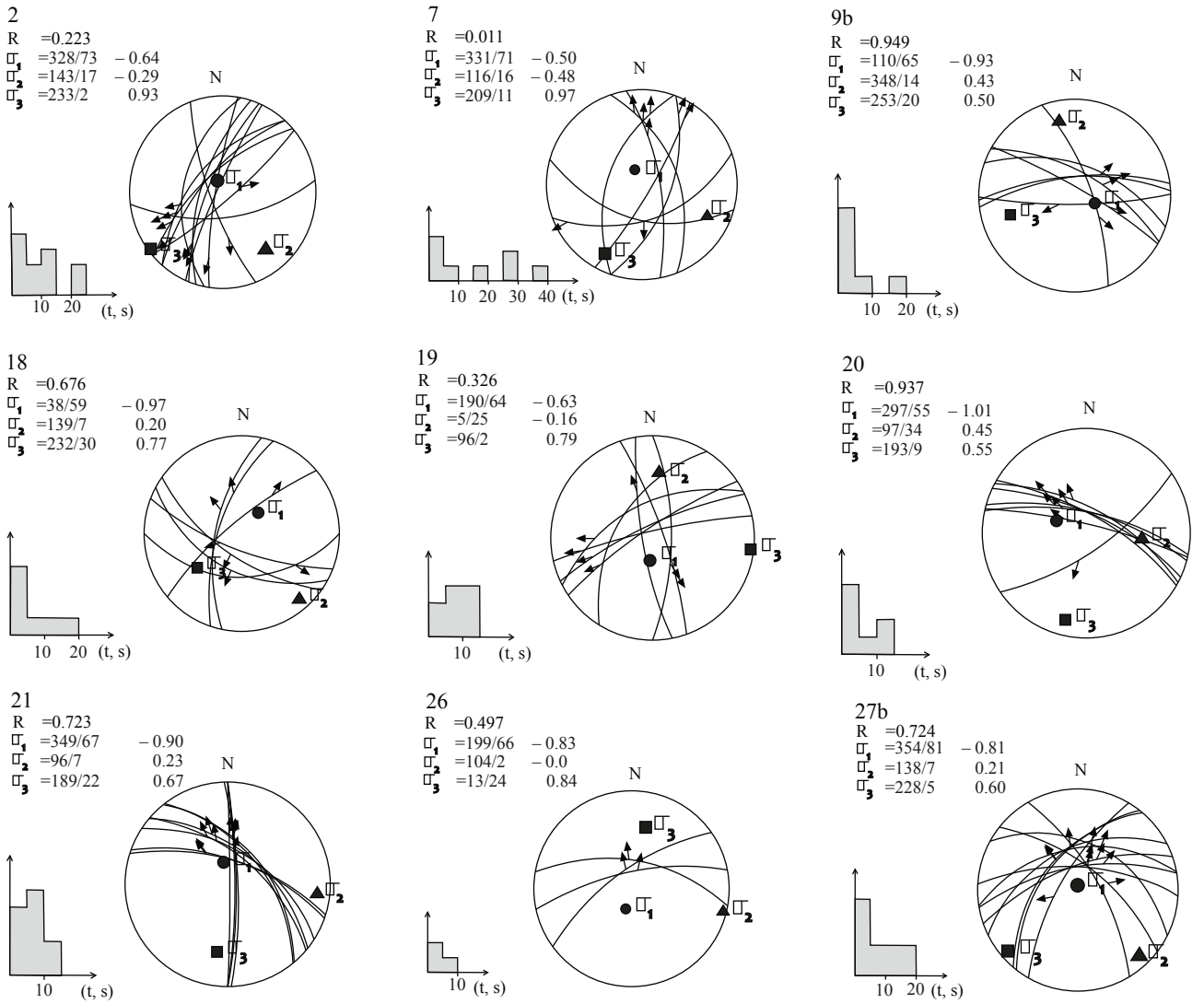

Figure 7. Lower hemisphere stereoplots showing a normal faulting mechanism under NNE–SSW extensional tectonic regime (SS.3) results shown in Table 2d. Histogram shows distribution of deviation angles (angle between the observed slip, s, the predicted slip, t).

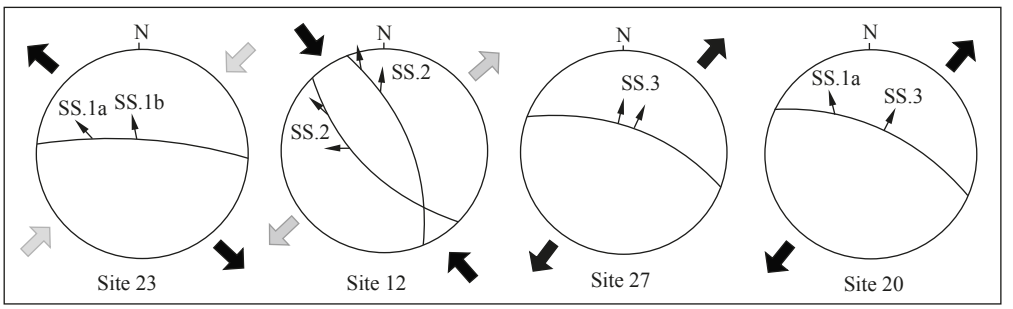

Figure 8. Chronology and cross-cutting (overlapping) relationships between different families of slip-vectors measured on fault planes at several sites. Fault planes and measured striations are shown in a lower hemisphere stereographic projection, arrows point in the horizontal slip azimuth direction presented by a tectonic regime (SS.1 a-b, SS.2, and SS.3) on sites 12, 20, 23, and 27.

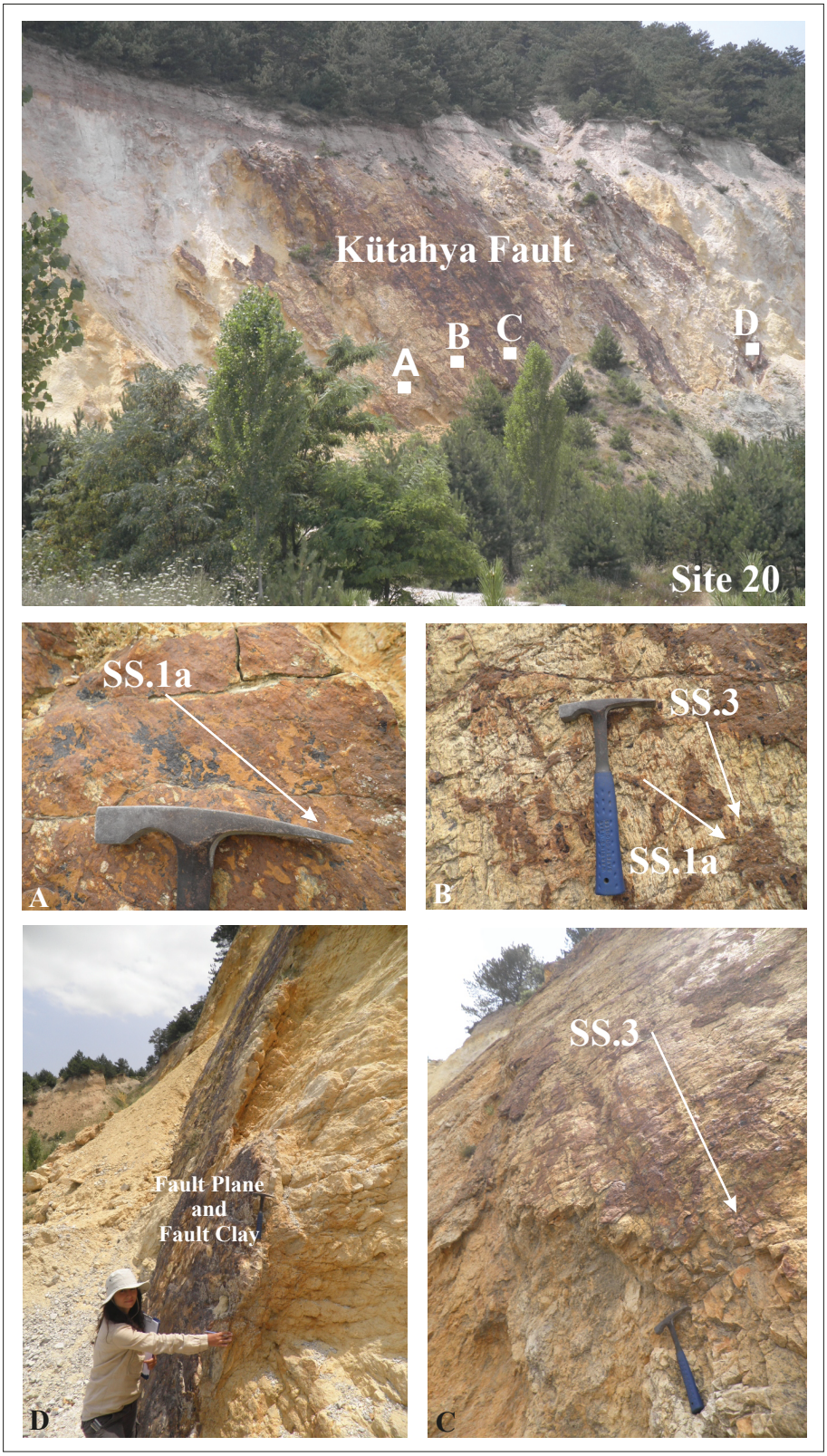

Figure 9. A main fault plane of the Kütahya Fault around the city of Kütahya in site 20 (the location of the photo is shown in Figure 3). A) Slickenlines showing the SS.1a tectonic regime. B) Superimposed slickenlines showing both SS.1a tectonic regime and SS.3 tectonic regime. C) Slickenlines showing the SS.3 recent tectonic regime. D) The view of fault plane and fault clay due to faulting.

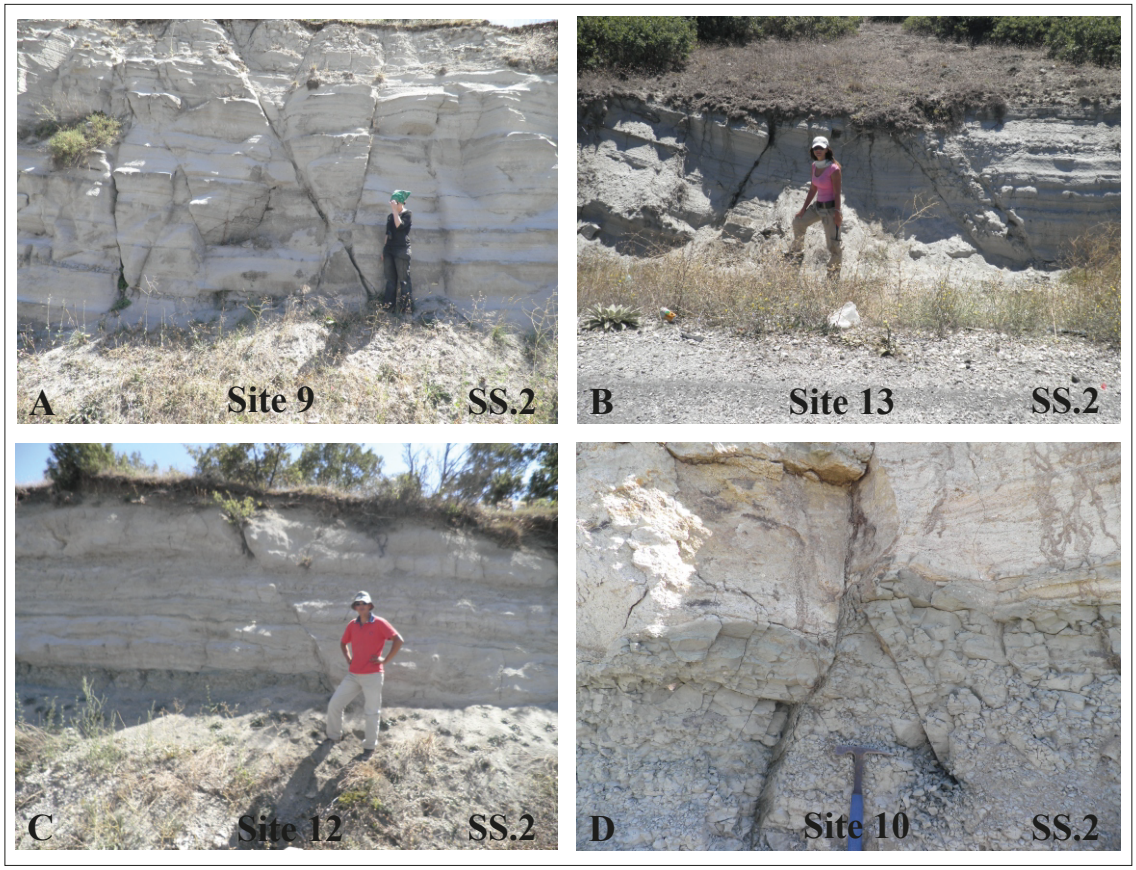

Figure 10. Examples of strike-slip faults with normal component under NW–SE compressional tectonic regime (SS.2) in sites 9, 10, 12, and 13 (the location of the photo is shown in Figure 3).

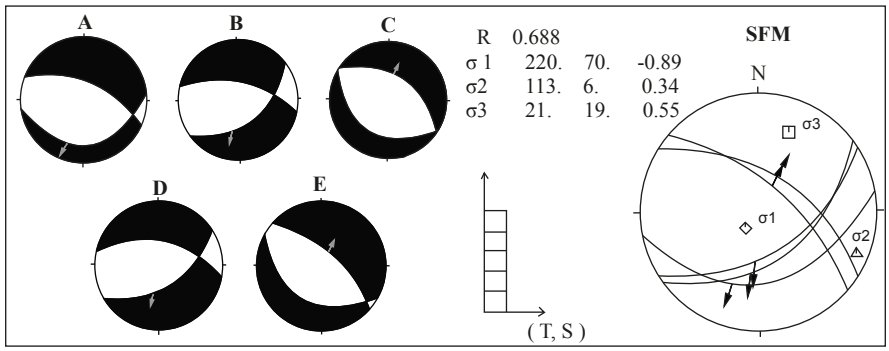

Figure 11. The lower hemisphere result (SFM) of the source mechanism inversion of 5 (A–E) earthquakes (references and detailed information for each earthquake given in Table 3). Seismic fault showing a gray arrow on each focal mechanism solution.

To determine the current tectonic regime along the Kütahya Fault, the numerical method developed by Carey-Gailhardis and Mercier (1987) was used. The common inversion solutions of these earthquakes found the smallest principle axis (σ_3) and intermediate principle axis (σ_2) are horizontal, while the largest principle axis (σ_1) is vertical, indicating an extensional regime with normal faulting. The smallest principle stress axis (σ_3) was 21°/19°. The Rm ratio was 0.68, showing this regime is represented by a triaxial stress tensor.

These results lead to the conclusion that the extensional orientation in the region is N 21° E (σ_3). The

Table 3. Parameters of focal mechanism solution for earthquakes (Boğaziçi University open access data) occurring in the study area presented in Figure 11.

Earthquakes	Date Day.Month. Year	Local time (UTC)	Latitude N (°)	Longitude E (°)	Plane 1 Strike°/Dip°/ Plunge°	Plane 1 Strike°/Dip°/ Plunge°	Mag. (Mw)	h (km)	Variance reduction (%)	Station number	References
A	28.06.2014	09.17	39.36	30.12	292°/65°/–76°	81°/28°/–119°	2.9	8	62.29	6	This study
B	18.04.2013	02:58	39.54	29.76	283°/57°/–58°	54°/44°/–130°	3.5	34	55.99	7	This study
C	15.03.2011	09:42	39.71	29.41	303°/53°/–88°	120°/37°/–92°	2.5	6	59.70	3	This study
D	05.07.2010	09:24	39.49	30.08	58°/50°/–121°	281°/49°/–59°	3.3	20	63.08	4	This study
E	22.08.2004	21:19	39.21	30.25	311°/63°/–84°	119°/28°/–101°	4.2	40	81.37	6	This study

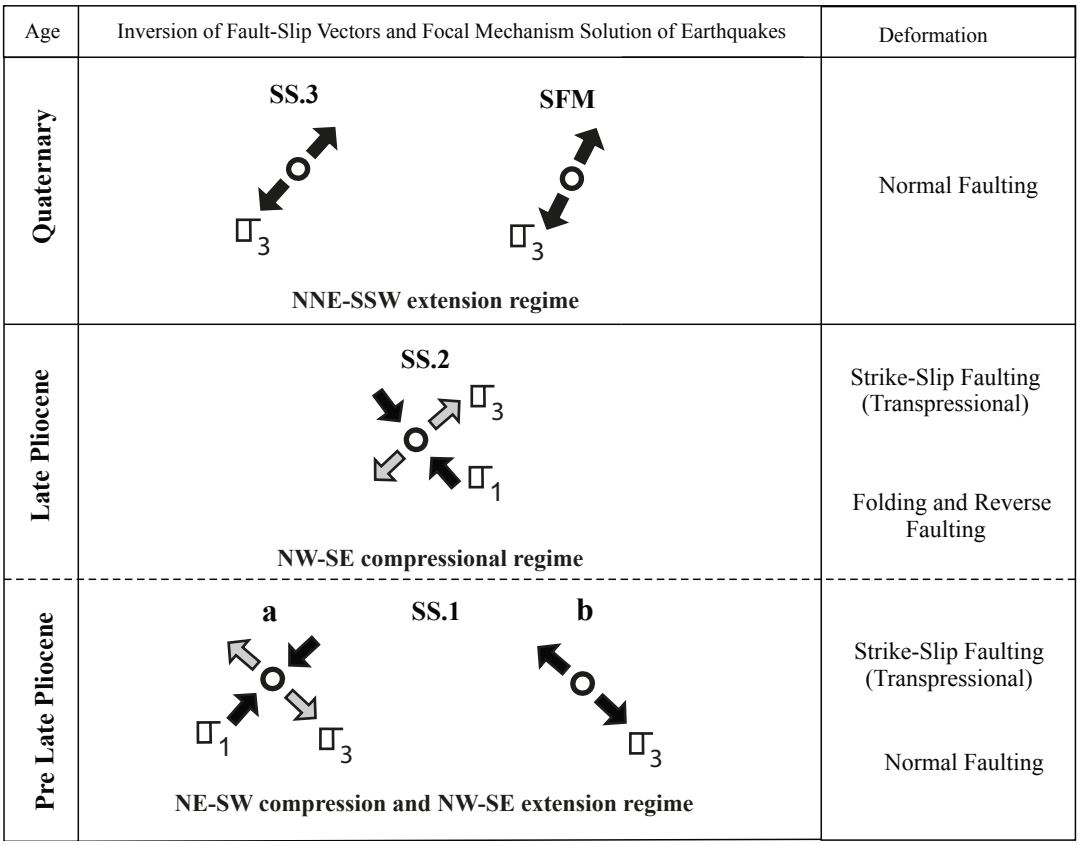

Figure 12. Distribution and results of Late Cenozoic stress states along the Kütahya Fault.

extensional regime with NNE–SSW orientation (SFM) is in accordance with the extensional direction obtained for the last tectonic regime (SS.3) from the kinematic analysis studies of fault assemblages and has the same orientation as the currently effective extensional direction in western–SW Anatolia.

4. Discussion and conclusion

This study was conducted with the aim of determining the stress situation and kinematic evolution in the Late Cenozoic of the Kütahya Fault and surrounding area. The Kütahya Fault has a WNW–ESE trend over nearly 40 km in length, presenting a clear morphology bounding the south of the Kütahya Basin. Data were obtained from planes clearly showing fault plane parameters along the Kütahya Fault and numerically analyzed.

The results of numerical analysis studies determined three main regional stress states (SS.1, SS.2, and SS.3) belonging to before the Late Pliocene, the Late Pliocene, and Quaternary periods. The study area was affected by a NE–SW compressional regime (SS.1a) in the period before the Late Pliocene, developing strike-slip faults and

folds that worked together with normal faults developed under a compatible NW–SE extensional regime (SS.1b). In the Late Pliocene in the region it appears a short-term and local NW–SE oriented compressional regime (SS.2) developed. The products of this regime are shear zone deformation together with right and left lateral strike-slip faults. Immediately before the Late Pliocene, the Kütahya Fault began to form for the first time, developing with left lateral strike-slip fault characteristics under a NE–SW compressional regime (SS.1a), and showed normal fault character under a regional NNE–SSW extensional regime after a regime change in the Quaternary (SS.3). Inversion of the earthquake focal mechanism solution produced similar results. This last tectonic regime of extension in the region is currently active (Figure 12). In light of the obtained data, the Kütahya Fault began motion as a left lateral strike-slip fault in a time (?) before the Late Pliocene and currently continues motion as a normal fault under the extensional regime. These Late Cenozoic tectonic regimes were determined by earthquakes together with numerical calculation methods for the first time for this fault and close surroundings.

The observed tectonic regime changes along the Kütahya Fault are still debated by researchers working in the region. Dewey and Şengör (1979) attempted to explain the initial E–W compressional regime and later N–S extensional regime with a comparative model for Western Anatolia. According to this model, with the collision of the Arabian plate in the east the Anatolian Block was prevented from moving west by the Hellenic Shear Zone. This obstacle to the lateral strike slip system caused east–west compression in Western Anatolia. This compression in continental crust thickened by previous orogenic events caused N–S extension on E–W oriented normal faults instead of causing north–south thrusting and thickening. In other words, E–W compression was countered with N–S extension. In this N–S extension the effect of the Cyprus Arc was great (Dewey and Şengör, 1979; Şengör et al., 2008). Thus, the Kütahya Fault with motion beginning under a compressional regime and later continuing as a normal fault under an extensional regime may be considered a product of the neotectonic evolution of Western Anatolia in accordance with other neotectonic stages and elements.

In the region the compressional regime before the Late Pliocene period determined in our kinematic analysis and the accompanying NW–SE extensional regime created the nearly NNE–SSW oriented Selendi and Demirci Basins. These basins are structural elements created under the effects of the old tectonic regime. However, contrary to the Selendi and Demirci basins, the WNW–ESE oriented Eskişehir, Kütahya, Simav, and Gediz basins obtained their final shape under the currently effective NNE–SSW extensional regime.

Acknowledgments

This work was financially supported by TÜBİTAK-ÇAYDAG (Project No: 109Y103) prepared as a master's thesis. The authors would like to thank Catherine Yiğit for professional editing assistance with English exposition that improved earlier versions of the text. We also thank the editor and anonymous reviewers for their valuable comments and suggestions, which improved the quality of the manuscript.

References

Alçiçek MC, Kazancı N, Özkul M (2005). Multiple rifting pulses and sedimentation pattern in the Çameli Basin, Southwestern Anatolia, Turkey. Sedimentary Geology 173: 409-431.

Al-Lazki A, Seber D, Sandvol E, Türkelli N, Mohamad R, Barazangi M (2003). Tomographic Pn velocity and anisotropy structure beneath the Anatolian plateau (eastern Turkey) and the surrounding regions. Geophysical Research Letters 30.

Altınok S, Karabacak V, Yalçıner CÇ, Bilgen N, Altunel E, Kıyak NG (2012). Kütahya Fay Zonu'nun Holosen aktivitesi. Türkiye Jeoloji Bülteni 55: 1: 1-17.

Ambraseys NN, Tchalenko JS (1972). Seismotectonic aspects of the Gediz, Turkey, Earthquake of March 1970. Geophysical Journal of the Royal Astronomical Society 30: 229-252.

Angelier J, Dumont JF, Karamanderesi H, Poisson A, Şimşek S et al. (1981). Analyses of fault mechanisms and expansion of Southwestern Anatolia since the Late Miocene. Tectonophysics 75: 1-9.

Arpat E, Şaroğlu F (1972). The East Anatolian fault system: thoughts on its development. Bulletin of the Mineral Research and Exploration 78: 33-39.

Barka A (1992). The North Anatolian Fault Zone. Annales Tecton 6: 164-195.

Barka A, Reilinger R (1997). Active tectonics of the Eastern Mediterranean region: deduced from GPS, neotectonic and seismicity data. Annali di Geofisica 40 (3): 587-610.

Bilim F (2007). Investigations into the tectonic lineaments and thermal structure of Kutahya–Denizli region, western Anatolia, from using aeromagnetic, gravity and seismological data. Physics of the Earth and Planetary Interiors 165: 135-146.

Biryol CB, Beck SL, Zandt G, Özacar AA (2011). Segmented African lithosphere beneath the Anatolian region inferred from teleseismic P-wave tomography. Geophysical Journal International 184: 1037-1057.

Bozkurt E (2001). Late Alpine evolution of the Central Menderes Massif, Western Anatolia, Turkey. International Journal of Earth Sciences 89: 728-744.

Bozkurt E (2003). Origin of NE trending basins in Western Turkey. Geodinamica Acta 16: 61-81.

Carey E (1979). Recherche des directions principales de contraintes associées au jeu d'une population de failles. Revue Geological Dynamic and Géography Physic 21: 57-66.

Carey-Gailhardis E, Mercier JL (1987). A numerical method for determining the state of stress using focal mechanisms of earthquake populations. Earth Planet Sci Lett 82: 165-179.

Cohen HA, Dart C, Akyüz HS, Barka A (1995). Syn-rift sedimentation and structural development of the Gediz and Büyük Menderes Grabens, Western Turkey. Geological Society of London 152: 629-638.

Demirci A, Özden S, Bekler T, Kalafat D, Pınar A (2015). An active extensional deformation example: 19 May 2011 Simav earthquake (Mw=5.8), Western Anatolia, Turkey. Journal of Geophysics and Engineering 12 (4): 525-565.

Dewey JF (1988). Extensional collapse of orogens. Tectonics 7 (6): 1123-1139.

Dewey JF, Şengör AMC (1979). Aegean and surrounding regions: complex multiplate and continuum tectonics in a convergent zone. Geological Society America Bulletin 90: 84-92.

Dreger DS (2002). Manual of the time-domain moment tensor inverse code (TDMT-INVC), release 1.1. Berkeley Seismological Laboratory Berkeley, 18.

Dumont JF, Uysal S, Şimşek S, Karamanderesi H, Letouzey J (1979). Formation of the grabens in Southwestern Anatolia. Bulletin of Mineral Research and Exploration Institute 92: 7-18.

Emre Ö, Doğan A, Özalp S (2013). 1:250000 scale active fault map series of Turkey. General Directorate Mineral Research and Exploration, Ankara, Turkey.

Erkul F, Tatar Erkul S, Manap HS, Çolak C (2017). An extensional and transtensional origin of elongated magmatic domes and localised transfer faults in the northern Menderes metamorphic core complex, western Turkey. Geodinamica Acta, 29: 1: 139-159.

Faccenna C, Bellier O, Martinod J, Piromallo C, Regard V (2006). Slab detachment beneath eastern Anatolia: a possible cause for the formation of the North Anatolian fault. Earth and Planetary Science Letters 242: 85-97.

Faccenna C, Piromallo C, Crespo Blanc A, Jolivet L, Rossetti F (2004). Lateral slab deformation and the origin of the arcs of the western Mediterranean. Tectonics 23: TC1012.

Göğüş OH, Pysklywec RN, Corbi F, Faccenna C (2011). The surface tectonics of mantle lithosphere delamination following ocean lithosphere subduction: insights from physical-scaled analogue experiments. Geochemistry, Geophysics, Geosystems 12.

Gürer ÖF, Özburan M, Sangu E, Doğan B (2005). Kütahya dolayının Neotektonik incelemesi. Kocaeli Üniversitesi Mühendislik Fakültesi Jeoloji Mühendisliği Bölümü BAP-Proje, No: 2005/14.

Gündoğdu E, Özden S, Güngör T (2015). Simav (Kütahya) ve yakın civarının Geç Senozoyik yaşlı jeodinamik evrimi. Türkiye Jeoloji Bülteni 58: 3: 23-38.

Jackson J, McKenzie DP (1988). The relationship between plate motion and seismic moment tensors, and the rates of active deformation in the Mediterranean and Middle-East. Geophys. J R Ast Soc 93: 45-73.

Jolivet L, Faccenna C, Huet B, Labrousse L, Le Pourhiet L et al. (2013). Aegean tectonics: strain localisation, slab tearing and trench retreat. Tectonophysics 597: 1-33.

Jolivet L, Brun JP (2010). Cenozoic geodynamic evolution of the Aegean. International Journal Earth Science (Geol Rundsch) 99: 109-138.

Karasözen E, Nissen E, Bergman EA, Johnson K L, Walters RJ (2016). Normal faulting in the Simav graben of western Turkey reassessed with calibrated earthquake relocations. Journal of Geophysical Research-Solid Earth 121: 6: 4553-4573.

Ketin İ (1948). Uber die tektonisch-mechanischen Folgerungen aus den grossen anatolischen Erdbeden des letzten Dezenniums. Geologische Rundchau 36: 77-83.

Koçyiğit A (1984). Güneybatı Türkiye ve Yakın Dolayında Levha İçi Yeni Tektonik Gelişim. Türkiye Jeoloji Kurumu Bülteni 27: 1-16.

Koçyiğit A, Bozkurt E (1997). Kütahya-Tavşanlı çöküntü alanının Neotektonik özellikleri. TUBİTAK Araştırma Projesi, No: YDABÇAG-126, 78.

Koçyiğit A, Yusufoğlu H, Bozkurt E (1999). Evidence from the Gediz Graben for episodic two-stage extension in Western Turkey. Journal of the Geological Society, London 156: 605-616.

Komut T, Gray R, Pysklywec R, Göğüş OH (2012). Mantle flow uplift of western Anatolia and the Aegean: interpretations from geophysical analyses and geodynamic modeling. Journal of Geophysical Research-Solid Earth 117.

Konak N (2002). 1/500.000 ölçekli Türkiye Jeoloji Haritasi İzmir paftası. MTA, Ankara, Turkey.

Le Pichon X, Angelier J (1979). The Hellenic arc and trench system: a key to the evolution of the eastern Mediterranean area. Tectonophysics 60: 1-42.

Le Pichon X, Angelier J (1981). The Aegean Sea. Philosophical Transactions of the Royal Society London A300: 357-372.

McClusky S, Balassanian S, Barka A, Demir C, Ergintav S et al. (2000). Global Positioning System constraints on plate kinematics and dynamics in the eastern Mediterranean and Caucasus. Journal of Geophysical Research 105: B3: 5695-5719.

Mercier JL (1981). Extensional–compressional tectonics associated with the Aegean Arc: comparison with the Andean Cordillera of South Peru–North Belivia. Philosophical Transactions of the Royal Society London A 300: 337-355.

Mercier JL, Carey E, Sebrier M (1991). Paleostress determinations from fault kinematics: application to the Neotectonics of the Himalayas–Tibet and the Central Andes. Philosophical Transactions of the Royal Society, London A 337: 41-52.

Mercier JL, Delibassis N, Gauthier A, Jarrige JJ, Lemeille F et al. (1979). La néotectonique de l'Arc Egéen. Rev Geol Dyn Geogr Phys, Paris 21: 67-92.

Mutlu AK, Karabulut H (2011). Anisotropic Pn tomography of Turkey and adjacent regions. Geophysical Journal International 187 (3): 1743-1758.

Över S, Özden S, Pınar A, Yılmaz H, Kamacı Z et al. (2016). Late Cenozoic stress state distributions at the intersection of the Hellenic and Cyprus Arcs, SW Turkey. Journal of Asian Earth Sciences 132: 94-102.

Över S, Özden S, Pınar A, Yılmaz H, Ünlügenç UC et al. (2010). Late Cenozoic stress field in the Çameli Basin, SW Turkey. Tectonophysics 492 (1-4): 60-72.

Över S, Özden S, Yılmaz H, Pınar A, Ünlügenç UC et al. (2013a). Plio-Quaternary stress regime in Eşen Çay Basin, SW Turkey. Geological Development of Anatolia and the Easternmost Mediterranean Region. Geological Society of London, London, Special Publications 372: 547-560.

Över S, Yılmaz H, Pınar A, Özden S, Ünlügenç UC et al. (2013b). Plio-Quaternary stress states in Burdur Basin, SW-Turkey. Tectonophysics 588: 56-68.

Özburan M (2009). Kütahya ve Çevresinin Neotektonik Özellikleri. PhD, Kocaeli University, Kocaeli, Turkey.

Özburan M, Gürer ÖF (2012). Late Cenozoic polyphase deformation and basin development, Kütahya region, western Turkey. International Geology Review 54: (12): 1401-1418.

Özden S, Gündoğdu E, Bekler T (2015). Interactions between Eurasian/African and Arabian plates: Eskişehir Fault, NW Turkey. Journal of African Earth Science 11: 349-362.

Piromallo C, Morelli A (2003). P wave tomography of the mantle under the Alpine-Mediterranean area. Journal of Geophysical Research-Solid Earth 108: B2.

Roberts GP, Ganas A (2000). Fault-slip directions in central and southern Greece measured from striated and corrugated fault planes: comparison with source mechanism and geodetic data. Journal of Geophysical Research-Solid Earth 105: B10: 23443-23462.

Şaroğlu F, Emre Ö, Boray A (1992). Türkiye'nin Aktif Fayları ve Depremsellikleri. Maden Tetkik Arama Genel Müdürlüğü, Ankara, Turkey.

Şengör AMC (1987). Tectonics of the Tethysides: orogenic collage development in a collisional setting. Annual Review Earth Planetary Science 15: 213-244.

Şengör AMC, Özeren S, Genç T, Zor E (2003). East Anatolian high plateau as a mantle-supported, north-south shortened domal structure. Geophys Res Lett 30 (24): 8045.

Şengör AMC, Özeren MS, Keskin M, Sakınç M, Özbakır AD, Kayan İ (2008). Eastern Turkish high plateau as a small Turkic-type orogen: implications for post-collisional crust-forming processes in Turkic-type orogens. Earth-Science Review 90 (1-2): 1-48.

Şengör AMC, Yılmaz Y (1981). Tethyan evolution of Turkey: a plate tectonic approach. Tectonophysics 75: 181-241.

Seyitoğlu G, Scott B (1991). Late Cenozoic crustal extension and basin formation in west Turkey. Geology Magazine 128: 155-166.

Seyitoğlu G, Scott B (1992). The age of the Buyuk Menderes Graben (Western Turkey) and its tectonic implications. Geology Magazine 129: 239-242.

Tokay F, Altunel E (2005). Eskişehir Fay Zonu'nun İnönü-Dodurga çevresinde Neotektonik aktivitesi. M.T.A. Dergisi 130: 1-15.

Wdowinski S, Ben-Avraham Z, Arvidson R, Ekstrom G (2006). Seismotectonics of the Cyprian Arc. Geophysical Journal International 164: 176-181.

Wortel MJR, Spakman W (2000). Subduction and slab detachment in the Mediterranean-Carpathian region. Science 290: 1910-1927.

Yılmaz Y, Genç SC, Gürer OF, Bozcu M, Yılmaz K et al. (2000). When did the Western Anatolian grabens begin to develop? In: Bozkurt E, Winchester JA, Piper JDA (editors), Tectonics and Magmatism in Turkey and the Surrounding Area. Geological Society Special Publication, Geological Society, London 173: 353-384.

Zanchi A, Angelier J (1993). Seismotectonics of western Anatolia: regional stress orientation from geophysical and geological data. Tectonophysics 222: 259-274.